SIR ANALYSIS IN SQUARE-SHAPED INDOOR PREMISES

A. Samuylov[†], D. Moltchanov[†], Yu. Gaidamaka[*], V. Begishev[*], R. Kovalchukov[*], P. Abaev[*], S. Shorgin[‡]
[*]Peoples' Friendship University of Russia, Moscow, Russia,
Email: {ygaidamaka, vobegishev, rnkovalchukov, pabaev}@sci.pfu.edu.ru
[†]Tampere University of Technology, Tampere, Finland,
Email: {andrey.samuylov, dmitri.moltchanov}@tut.fi
[‡]Federal Research Center "Computer Science and Control" of the Russian Academy of Sciences, Moscow, Russia,
Email: sshorgin@ipiran.ru

KEYWORDS

Wireless networks, signal-to-interference ratio, distributions, indoor propagation, square cells, wall penetration

ABSTRACT

The increased wireless network densification has resulted in availability of wireless access points (AP) in almost each and every indoor location (room, office, etc.). To provide complete in-building coverage very often an AP is deployed per room. In this paper we analyze signal-to-interference (SIR) ratio for wireless systems operating in neighboring rooms separated by walls of different materials by explicitly taking into account the propagation and wall penetration losses. Both AP and direct device-to-device (D2D) configurations are addressed. Our numerical results indicate that the performance of such system is characterized by both the loss exponent describing the propagation environment of interest and wall materials. We provide the numerical results for typical wall widths/materials and analyze them in detail.

INTRODUCTION

The predicted increase in the user traffic demands places extreme requirements on the future evaluation of mobile systems, often referred to as fifth generation (5G) networks [1], [2]. In addition to physical layer improvements including advanced modulation and coding and MIMO techniques, over the last decade researchers investigated a number of network solutions providing decisive performance improvements including the use of small (micro/pico/femto) cells [3], client-relays [4], direct in-band and out-of-band device-to-device communications [5]. All these concepts target aggressive spatial reuse of frequencies promising substantial area capacity gains.

With the adoption of novel mechanism the user devices are expected to take a more active part in 5G systems and, in some cases, even take on the role of the network infrastructure in providing wireless connectivity such as offering D2D-based data relaying, proximity services, etc. This shift from the classic cellular model is dictated by the progress in communications technologies: the user devices are augmenting their capabilities, whereas the base stations (BSs) are becoming smaller as a result of the ongoing network densification [6].

The networks densification, novel networking and service mechanisms as well as the trend to use multiple access technologies to serve the users, known as heterogeneous cellular system concept, altogether lead to increased randomness of the network, where the positions of servicing stations such as BSs, relays and D2D partners are random rather than deterministic.

The signal-to-interference ratio (SIR) is a universal metric specifying performance of wireless systems [7]. Once SIR is known one could describe the Shannon rate of the channel and spectral efficiency of the system. In contrast to noise-limited systems, where the bit error rate (BER) decreases exponentially with signal-to-noise ratio (SNR), the heterogeneous mobile networks are interference-limited showing linear improvement of BER with respect to SIR. Thus, the increase of the emitted power does not improve the performance of these systems. Thus, the problem of finding SIR for typical network configurations is of special importance characterizing applicability and typical scenarios of modern and future wireless technologies.

The SIR performance of wireless systems is often studied using the tools of stochastic geometry [8]. The basic approach is to specify the point process on the plane modeling positions of the stations and then derive the interference at the point of interest. The last step is rather complex as we need closed-form distribution of distance to the point of interest from at least several neighboring points. For this reason typical considered models are often limited to Poisson point process on the plane for which we immediately have closed-form expressions for distributions of distances to the i-th neighbor [9].

The constantly increasing need for wireless connectivity on-the-go [10] are gradually changing the way service is provisioned in wireless networks. Nowadays, one of the trends is to deploy small wireless stations including both IEEE 802.11 or micro-LTE access points (AP) in crowded areas to benefit from increased network densification [6] and shorter propagation distances. Examples include large shopping mall, office environment, where one of few adjacent rooms is served by an AP having relatively small coverage area. In this dense environment interference between neighboring APs is inevitable and may easily lead to degraded system performance.

In this paper, using the tools of stochastic geometry, we analyze performance of wireless systems operating in neighboring rooms of rectangular configuration. We consider both direct device-to-device and AP configurations assuming that

Proceedings 30th European Conference on Modelling and Simulation ©ECMS Thorsten Claus, Frank Herrmann, Michael Manitz, Oliver Rose (Editors)
ISBN: 978-0-9932440-2-5 / ISBN: 978-0-9932440-3-2 (CD)

the systems in adjacent rooms operate at the same frequency. The analytical results are compared to simulations showing adequate agreement. Numerical results for the set of input metrics demonstrate that the system performance is dictated by the interplay between path loss exponent typical for a given environment and type of the walls used between rooms.

The rest of the paper is organized as follows. First, in the next section we introduce a system model. Further, we analytically study SIR for downlink scenario. The simulation models for both downlink and D2D scenarios are introduced next. Numerical results for different sets in input variables are illustrated. Conclusions are drawn in the last section.

SYSTEM MODEL

In this study we focus on an indoor scenario with grid aligned rooms, see Fig. 1 that are typical for shopping malls or office buildings. In these environments rooms are often of rectangular or square shapes. Each room is assumed to be equipped with an AP deployed in the geometrical center. To take advantage of the wireless network densification trend as a solution to upgrade the degree of spatial reuse, the devices in adjacent rooms are assigned the same set of communication channels [6]. The mobile terminals (users) operating over the same channel are assumed to be uniformly distributed over the room, one per room. We concentrate on the so-called tagged user in the central room, see Fig. 1(a) and Fig. 1(b). We assume both AP and users to be equipped with omni-directional antennas. We do not focus on a particular radio technology addressing the general case.

In addition to AP scenario we also address D2D configuration, sketched in Fig. 1(c). The principal difference compared to AP case is that both transmitter and receiver are assumed to be uniformly distributed within a room. Under this assumption the configuration is symmetric, i.e., we do not have to distinguish between uplink and downlink cases. Similarly, we concentrate on D2D pair located in the central room.

Focusing on SIR, as a metric of interest, for both AP and D2D configurations we calculate it for a randomly chosen receiving device, taking into account the interference from a set of neighboring rooms. Using the commonly used propagation model, we add a correction factor, accounting for the attenuation of a signal when passing through a wall

$$SIR = \frac{S}{\sum\limits_{i=1}^{N} (I_i B_i)}, \tag{1}$$

where S is the received signal power, N is the number of interfering sources, I_i is the interference power from the i^{th} source, B_i is the correction factor.

The received signal power is a function of the distance between the transmitter and the receiver (or between the interfering device and the device of interest). The functions in (1) are specified as

$$S = S(l) = g l^{-\gamma},\ I_i = I_i(l_i) = g {l_i}^{-\gamma}, \tag{2}$$

where g is the transmit power assumed to be constant for all the transmitters, l is the distance, and γ is the path loss exponent, which ranges from 2 to 6.

ANALYTICAL APPROACH

Uplink scenario

Consider the case with four interfering devices. Here we build an analytical model for Uplink scenario where devices are located in the square rooms with sides of $c = a_j = b_j,\ j = \overline{1,3}$, as shown in Fig. 1(a). Taking this into account, (1) can be simplified as

$$SIR = \frac{S(R_0)}{\sum\limits_{i=1}^{4} (I_i B_i)}, \tag{3}$$

$$S(R_0) = g R_0^{-\gamma}, \qquad \sum_{i=1}^{4} I_i (D_i B_i) = g \sum_{i=1}^{4} {D_i}^{-\gamma} B_i, \tag{4}$$

where R_0 is the distance between Tx_0 and Rx_0. The distance between Tx_i and Rx_0 is denoted by D_i. Assuming constant transmit power (3) reads as

$$SIR = \frac{g R_0^{-\gamma}}{g \sum\limits_{i=1}^{4} \left({D_i}^{-\gamma} B_i\right)} = \frac{R_0^{-\gamma}}{\sum\limits_{i=1}^{4} \left({D_i}^{-\gamma} B_i\right)}. \tag{5}$$

Introduce the following random variables

$$\xi = SIR,\ \eta_1 = R_0^{-\gamma},\ \eta_2 = D^{-\gamma}. \tag{6}$$

According to the method described in [11] the probability density function (pdf) of $D^{-\gamma}$, $W_{\eta_2}(y_2)$, is given by

$$W_{\eta_2}(y_2) = \left(\tfrac{2}{\gamma c^2}\ y_2^{\frac{-2}{\gamma}-1}\right) \times$$

$$\times \begin{cases} 0,\ y_2 \geq \left(\frac{c}{2}\right)^{-\gamma} \\ \arcsin\left[\frac{c}{2 y_2^{-1/\gamma}}\right] - \arcsin\left[\frac{\sqrt{-9c^1 + 4 y_2^{-2/\gamma}}}{2 y_2^{-1/\gamma}}\right], \\ \left(c\sqrt{\frac{5}{2}}\right)^{-\gamma} < y_2 \leq \left(\frac{3c}{2}\right)^{-\gamma} \\ \arcsin\left[\frac{\sqrt{-c^2 + 4 y_2^{-2/\gamma}}}{2 y_2^{-1/\gamma}}\right], \\ \left(\frac{c}{\sqrt{2}}\right)^{-\gamma} < y_2 \leq \left(\frac{c}{2}\right)^{-\gamma} \\ \arcsin\left[\frac{c}{2 y_2^{-1/\gamma}}\right], \\ \left(\frac{3c}{2}\right)^{-\gamma} < y_2 \leq \left(\frac{c}{\sqrt{2}}\right)^{-\gamma} \end{cases} \tag{7}$$

Consider now the total sum of all interfering signals. Since the convolution of (7) is not trivial, we approximate this sum with a Normal distribution. Using (7) we calculate the mean and variance of the interfering signal power as

$$\widetilde{\mu} = \sum_{i=1}^{4} \mu_i B_i,\ \widetilde{\sigma}^2 = \sum_{i=1}^{4} \sigma_i^2 B_i. \tag{8}$$

Since all four rooms are symmetric, the distributions of the individual interfering signals are the same. Assuming the same material and width for all walls between the room of interest and the interfering rooms, (8) is reduced to

$$\widetilde{\mu} = 4\mu B,\ \widetilde{\sigma}^2 = 4\sigma^2 B. \tag{9}$$

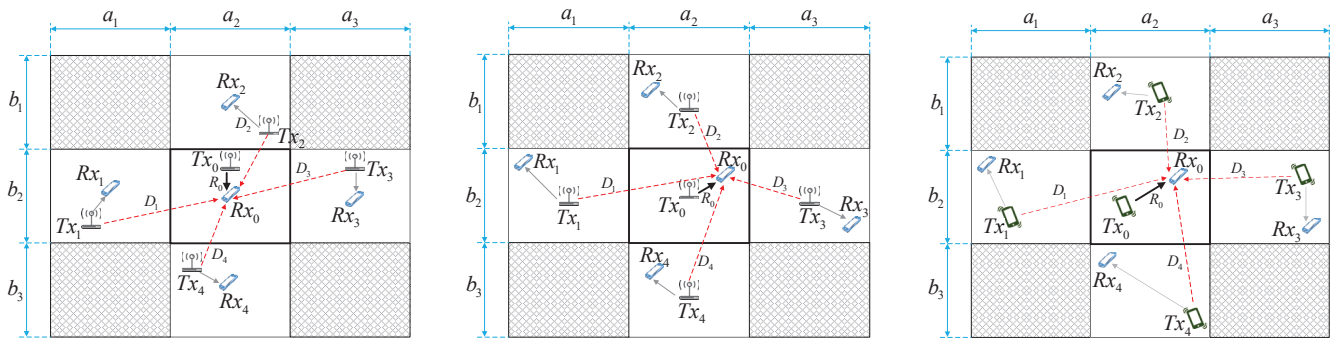

(a) Uplink scenario (b) Downlink scenario (c) D2D scenario

Fig. 1. Layout of the three considered scenarios.

The approximating Normal distribution is then written as

$$N_{\eta_2}(x) = \frac{1}{\widetilde{\sigma}\sqrt{2\pi}}\, e^{-\frac{(x-\widetilde{\mu})^2}{2\widetilde{\sigma}^2}} \quad . \tag{10}$$

The pdf of the signal of interest $W_{\eta_1}(y_1)$ is obtained as

$$W_{\eta_1}(y_1) = \left(\frac{2}{\gamma c^2} y_1^{\frac{-2}{\gamma}-1}\right) \times$$

$$\times \begin{cases} \pi, & \left(\frac{c}{2}\right)^{-\gamma} < y_1 < \infty \\ 2\left(\arcsin\left[\frac{c}{2y_1^{-1/\gamma}}\right] - \arcsin\left[\frac{\sqrt{-c^2+4y_1^{-2/\gamma}}}{2y_1^{-1/\gamma}}\right]\right), & \\ \left(\frac{c}{\sqrt{2}}\right)^{-\gamma} < y_1 \leq \left(\frac{c}{2}\right)^{-\gamma}. & \end{cases} \tag{11}$$

Now we derive the density function for (3) by applying the functional transformation of random variables [12]. We obtain the pdf of random variable ξ denoting the SIR based on the joint pdf of the signal power of interest and total interfering signal power. Recalling the form of SIR in (3), we establish

$$\begin{aligned} y_3 &= f(x_3, x_4) = x_3/x_4 \\ y_4 &= x_4, \end{aligned} \tag{12}$$

where y_4 is an auxiliary variable.

The inverse of (12) takes the following form

$$\begin{aligned} x_3 &= \varphi(y_3, y_4) = y_3 y_4, \\ \tfrac{\partial\, \varphi(y_3,y_4)}{\partial\, y_3} &= y_4. \end{aligned} \tag{13}$$

The pdf we are looking for is obtained using

$$\begin{aligned} &W_{\eta_1,\eta_2}(y_3, y_4) = \\ &= w_{\chi_1,\chi_2}\left(\varphi\left(y_3, y_4\right), y_4\right) \left|\tfrac{\partial\, \varphi(y_3,y_4)}{\partial\, y_3}\right|, \end{aligned} \tag{14}$$

where $w_{\chi_1,\chi_2}(y_3, y_4)$ is the joint density of $D^{-\gamma}$ and $\sum R_0^{-\gamma}$. To obtain a univariate density function of SIR we integrate out y_4 in (14)

$$\begin{aligned} &W_{\xi}(y_3) = \\ &= \int_{\mathbf{Y}} w_{\chi_1,\chi_2}\left(\varphi\left(y_3, y_4\right), y_4\right) \cdot \left|\tfrac{\partial\, \varphi(y_3,y_4)}{\partial\, y_3}\right| dy_4\,, \end{aligned} \tag{15}$$

where $\mathbf{Y}$ is the range of the variable y_4 for the inverse.

According to the limits imposed by (7, 10), $\mathbf{Y}$ is

$$\begin{aligned} &\left\{\left(\tfrac{c}{\sqrt{2}}\right)^{-\gamma} < y_1 \leq \left(\tfrac{c}{2}\right)^{-\gamma}, \quad -\infty < y_2 < \infty \right\} \cup \\ &\cup \left\{\left(\tfrac{c}{2}\right)^{-\gamma} < y_1 < \infty\,, \ -\infty < y_2 < \infty \right\}. \end{aligned} \tag{16}$$

Thus, we have

$$\mathbf{Y} = Y^1 \cup Y^2, \tag{17}$$

where

$$\begin{aligned} Y^1 = &\left\{y_3 < 0, \quad \tfrac{e^{\gamma \ln 2 - \gamma \ln c}}{y_3} < y_4 < \tfrac{e^{\frac{1}{2}\gamma \ln 2 - \gamma \ln c}}{y_3}\right\} \cup \\ &\cup \left\{y_3 > 0, \ \tfrac{e^{\frac{1}{2}\gamma \ln 2 - \gamma \ln c}}{y_3} < y_4 < \tfrac{e^{\gamma \ln 2 - \gamma \ln c}}{y_3} \right\}. \end{aligned} \tag{18}$$

and

$$\begin{aligned} Y^2 = &\left\{y_3 < 0, \quad y_4 < \tfrac{e^{\gamma \ln 2 - \gamma \ln c}}{y_3}\right\} \cup \\ &\cup \left\{y_3 > 0, \ y_4 > \tfrac{e^{\gamma \ln 2 - \gamma \ln c}}{y_3} \right\}. \end{aligned} \tag{19}$$

The density of SIR, $W_{\xi}(y_3)$, is now provided by

$$W_{\xi}(y_3) = \begin{cases} \int\limits_{M_1} I_1(y_3, y_4) dy_4 + \int\limits_{M_3} I_1(y_3, y_4) dy_4, y_3 < 0 \\ \int\limits_{M_2} I_2(y_3, y_4) dy_4 + \int\limits_{M_4} I_2(y_3, y_4) dy_4, y_3 \geq 0. \end{cases} \tag{20}$$

where the limits of integration are

$$\begin{aligned} M_1 &= \left\{(y_3, y_4) \ : \ \tfrac{e^{\gamma \ln 2 - \gamma \ln c}}{y_3} < y_4 < \tfrac{e^{\frac{1}{2}\gamma \ln 2 - \gamma \ln c}}{y_3}\right\} \\ M_2 &= \left\{(y_3, y_4) \ : \ \tfrac{e^{\frac{1}{2}\gamma \ln 2 - \gamma \ln c}}{y_3} < y_4 < \tfrac{e^{\gamma \ln 2 - \gamma \ln c}}{y_3}\right\} \\ M_3 &= \left\{(y_3, y_4) \ : \ y_4 < \tfrac{e^{\gamma \ln 2 - \gamma \ln c}}{y_3}\right\} \\ M_4 &= \left\{(y_3, y_4) \ : \ y_4 > \tfrac{e^{\gamma \ln 2 - \gamma \ln c}}{y_3}\right\} \end{aligned} \tag{21}$$

while the integrands have the following forms

$$I_1(y_3,y_4) = \\ = \frac{\arcsin\left[\frac{c}{2(y_3\cdot y_4)^{\frac{-1}{\gamma}}}\right] - \arcsin\left[\frac{\sqrt{-c^2+4(y_3\cdot y_4)^{\frac{-2}{\gamma}}}}{2(y_3\cdot y_4)^{\frac{-1}{\gamma}}}\right]}{\frac{4y_4}{\gamma c^2}(y_3\cdot y_4)^{\frac{-2}{\gamma}-1}\, e^{-\frac{(y_4-\tilde{\mu})^2}{2\tilde{\sigma}^2}}},$$

$$I_2(y_3,y_4) = \frac{2\sqrt{2\pi^3}\; y_4\cdot\tilde{\sigma}\,(y_3\cdot y_4)^{\frac{-2}{\gamma}-1}}{\gamma c^2\; e^{\left(-\frac{(y_4-\tilde{\mu})^2}{2\tilde{\sigma}^2}\right)}}. \qquad (22)$$

As we show in the numerical results section, this yields a pretty loose approximation due to the fact that we take into account the interference only from four sources, which is not large enough to comply with the central limit theorem. Thus, we compare the obtained results with another approximation based on the hyperexponential distribution. In this case we use the truncated two phase hyperexponential distribution to approximate the interference from a single source (7). The total interference power is obtained by convolving the obtained approximate distribution four times. We will omit the derivation, as the method we use to obtain these results is exactly the same like described in this section.

Downlink and D2D cases

The performed analysis for uplink scenario is feasible due to the independence of propagation paths between interferers and receiver. In downlink scenario these distances are no longer independent as all interference paths share the same fixed point - the receiver of interest. Because of this fact, the approximation for the denominator in (1) cannot be used without any further assumptions, thus complicating further derivations. Due to symmetric configuration of the scenario, one may observe that approximation obtained by assuming independence between these distances will result in significant approximation error. The situation is similar for D2D scenario, where the interference paths are again dependent. To facilitate derivation of the SIR densities in these cases we developed simulation environment described in the next section.

SIMULATION ENVIRONMENT

The developed simulation model based on the Monte Carlo method is a software tool implemented in C++ to gather statistics of SIR for a receiver in the central cluster by directly modeling all the underlying random variables. The tool relies on the same propagation model we used in analytical derivations, allowing not only to acquire SIR for downlink and D2D cases, but as well to assess the accuracy of analytical model.

The basic principle of the tool is as follows. We randomly choose all coordinates of devices that interfere and transmit signal to the target device located in the central cluster. Using SIR expression provided in (5) we collect statistics by repeating this process sufficiently many times. Once the statistics is obtained empirical pdf is constructed. Due to insignificant resource usage for all input values of interest we are able to obtain a number of samples that is significantly higher than recommended $n = 1 + \lfloor \log_2 N \rfloor$. All the characteristics of random variables have been obtained using conventional statistical methods.

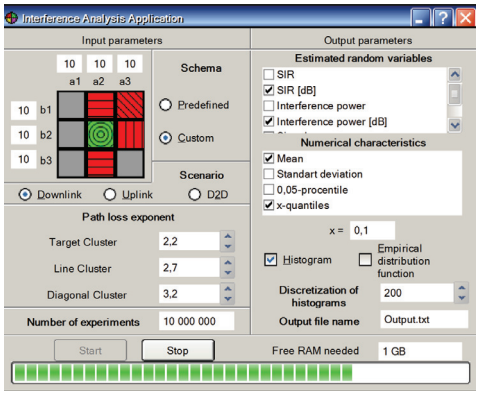

Fig. 2. Simulation tool graphical user interface.

The graphical user interface for Windows operating system is shown in Fig. 2. In the left pane user defines input parameters for modeling. They are the lengths of the sides of rectangular rooms and the value for the path loss exponent. An estimate of the SIR is obtained in either the so-called "standard" mode, when interference from all eight neighboring nodes is taken into account, or in the so-called "custom" mode, where the user manually selects the set of interfering rooms. Fig. 2 demonstrates an example of a user-mode selection.

The simulation model provides three options for the location of the devices in the clusters: the so-called "uplink" scenario, where the transmitters are located in the centers of rooms, and the coordinates of the receivers all follow uniform distribution, the "downlink" scenario, where the receivers are in the centers of their areas and coordinates of the transmitters follow uniform distribution, and the so-called "D2D" scenario, where the coordinates of both receivers and transmitters are distributed uniformly. In the right pane, a user sets the output parameters of the simulator. One or more characteristics can be chosen, including SIR, the power of the useful signal, the power of interfering signal, as well as their statistical characteristics. Particularly, when assessing SIR the 0.05-quantile is of special interest. The representation of the results can be selected by checking the box option "histogram" or "empirical distribution function". The last two parameters are responsible for setting the number of intervals of the histogram and the empirical pdf of random variables.

NUMERICAL RESULTS

In this section we present numerical results for all three considered scenarios. For uplink case we compare analytical data with those obtained using simulations. For comparison purposes, the numerical modeling was carried out in square clusters with sizes $c = 10$ (hereinafter the lengths are given in arbitrary units, e.g. meters), for all three scenarios. For downlink and D2D scenarios simulation data are presented. The values of losses caused by wall penetration are taken from [13]

Fig. 3 illustrates the comparison between analytical and simulation results for room size set to 10 and different path loss exponents. The number of samples used to construct

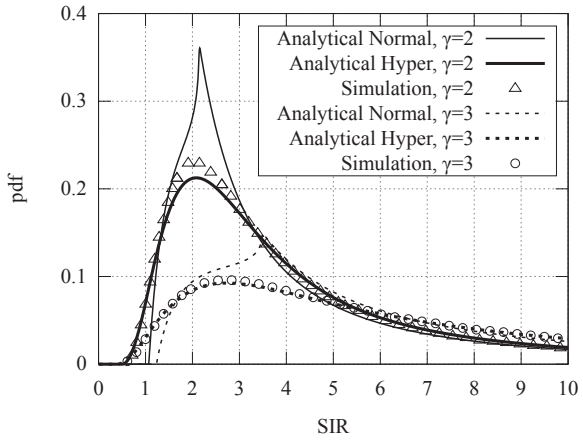

Fig. 3. Comparison of analytical and simulation results.

the empirical density function has been set to $10e6$. First, as one may notice, analytical results obtained by modeling the joint interference by Normal distribution deviate from the simulations implying that the model provides fairly loose approximation. The deviations is attributed to the approximation by the Normal distribution. Basically, it just shifts the distribution of the signal of interest (11), leaving the form intact. This is especially true for small values of SIR that are of special importance in practice specifying the so-called outage probabilities. However, the results obtained using Hyperexponential approximation for a single interferer yield a pretty tight fit for the empirical results and can be used as a lower bound estimate.

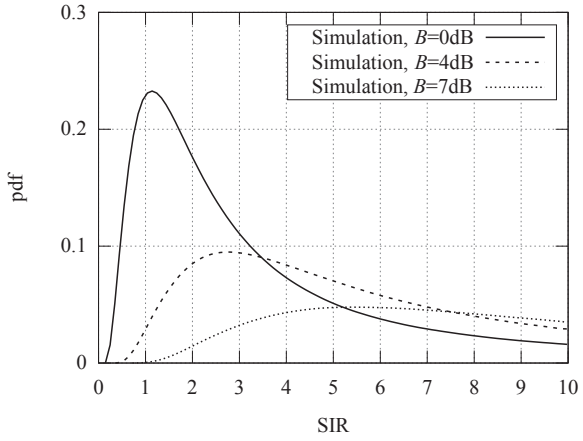

Fig. 4. SIR for uplink scenario, $c = 10$, $\gamma = 3$.

The comparison of SIR densities obtained using the simulation approach for $c = 10$ and path loss exponent $\gamma = 3$, is shown in Fig. 4. These figures were constructed assuming (i) no walls between rooms (loss of 0 dB, i.e. $B = 1$), (ii) wood walls with thickness 102mm resulting in (loss of 4 dB, i.e. $B \approx 0.4$), and (iii) brick walls of thickness 267mm corresponding to (loss of 4 dB, i.e. $B \approx 0.2$). As one may observe, the presence of walls between rooms fundamentally changes the structure of SIR density. As expected, the mode of the distribution shifts to the left implying better system performance.

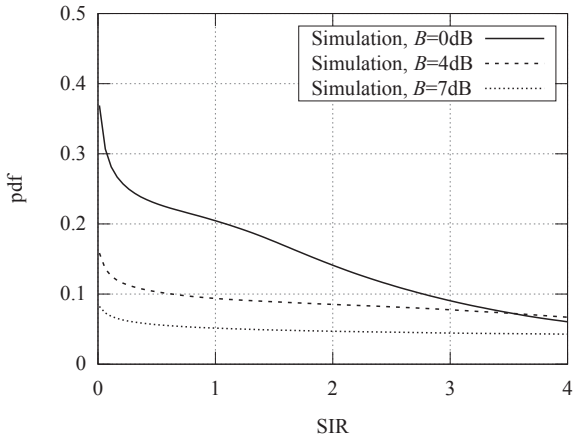

Fig. 5. SIR for downlink scenario, $c = 10$, $\gamma = 3$.

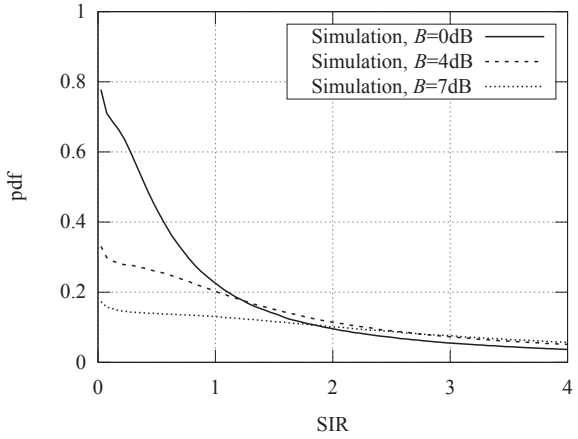

Fig. 6. SIR for D2D scenario, $c = 10$, $\gamma = 3$.

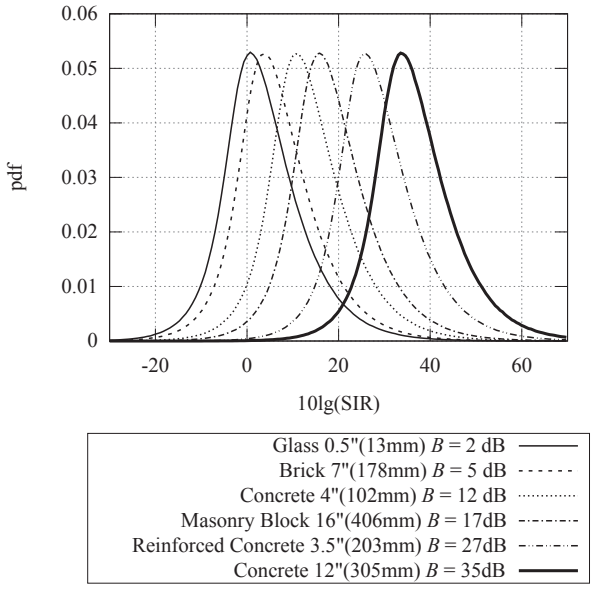

Fig. 7. SIR for a number of different wall materials.

For both downlink and D2D scenarios we obtained SIR densities using simulation approach. Fig. 5 compares SIR distributions for different path loss exponents and type of walls having c fixed at 10. Observing Fig. 4, where $\gamma = 3$, one may notice the "so-called" knees in the form of the densities. These bending points are not artifacts of the simulation study but are inherent form of the density corresponding to transition from small path loss exponent ($\gamma = 2$ and slightly greater) resulting in Gamma-like unimodal densities to high exponents around 4 characterized by distributions with no mode. Observe that the bending point gets smoother when the material of walls becomes harder to penetrate for electromagnetic radiation. For $\gamma = 4$ the densities are completely smooth implying that the wall material effect if similar to the increase of the path loss exponent.

The D2D case for different propagation loss exponents and $c = 10$ is shown in Fig. 6. For D2D scenario the form of the densities corresponds to $\gamma = 3$. As one may observe increasing the propagation losses caused by walls materials the mass of the density tends to concentrate on the left hand side making the tail of the distribution lighter. Thus, the propagation conditions become better.

Finally, the performance of the D2D connectivity for a number of different wall materials and path loss exponents is illustrated in Fig. 7. Here, the results are presented in dB using the transformation $10 \log_{10} I$. The data for propagation loss for different materials is taken from [14].

CONCLUSIONS

In this paper we analyzed performance of densely deployed indoor wireless systems for both D2D and AP configurations. For uplink AP configuration we obtained analytical results and demonstrated that for downlink AP and D2D configurations the interference path are, in fact, dependent preventing mathematical analysis in these cases. These scenarios have been addressed using simulation study.

Our results indicate that the performance of the considered scenarios is affected by the interplay between the propagation loss exponent and the types of walls between rooms. We evaluated the defined scenarios for a range of these parameters.

ACKNOWLEDGMENTS

The reported study was partially supported by RFBR, research projects No. 14-07-00090, 15-07-03051.

REFERENCES

[1] Ericsson, AB, "Ericsson mobility report," 2015.

[2] Cisco, "Cisco visual networking index: Global mobile data traffic forecast update, 2014-2019," 2015.

[3] J. Andrews, H. Claussen, M. Dohler, and S. Rangan, "Femtocells: Past, present, and future," *IEEE JSAC*, vol. 30, pp. 497–508, Apr. 2012.

[4] J. Lee, H. Wang, J. Andrews, and D. Hong, "Outage probability of cognitive relay networks with interference constraints," *IEEE Trans. Wir. Comm.*, vol. 10, pp. 390–395, Feb. 2011.

[5] G. Fodor, S. Parkvall, S. Sorrentino, P. Wallentin, Q. Lu, and N. Brahmi, "Device-to-device communications for national security and public safety," *IEEE Acess*, vol. 2, pp. 1510–1520, Apr. 2014.

[6] N. Bhushan, J. Li, D. Malladi, R. Gilmore, D. Brenner, A. Damnjanovic, R. Sukhavasi, C. Patel, and S. Geirhofer, "Network densification: the dominant theme for wireless evolution into 5G," *IEEE Communications Magazine*, vol. 52, no. 2, pp. 82–89, 2014.

[7] V. Sathya, A. Ramamurthy, S. Kumar, and B. Tamma, "On improving SINR in LTE hetnets with D2D relays," *Computer Communications*, 2015.

[8] J. G. Andrews, R. K. Ganti, M. Haenggi, N. Jindal, and S. Weber, "A primer on spatial modeling and analysis in wireless networks," *IEEE Communications Magazine*, vol. 48, no. 11, pp. 156–163, 2010.

[9] D. Moltchanov, "Survey paper: Distance distributions in random networks," *Ad Hoc Netw.*, vol. 10, no. 6, pp. 1146–1166, 2012.

[10] L. Zhou, "D2D communication meets big data: From theory to application," *Mobile Networks and Applications*, vol. 20, no. 6, pp. 783–792, 2015.

[11] A. Samuylov, A. Ometov, V. Begishev, R. Kovalchukov, D. Moltchanov, Y. Gaidamaka, K. Samouylov, S. Andreev, and Y. Koucheryavy, "Analytical performance estimation of network-assisted D2D communications in urban scenarios with rectangular cells," *Transactions on Emerging Telecommunications Technologies*, 2015.

[12] B. Levin, *Theoretical Foundations of Statistical Radio Engineering*. M.: Radio i Svyaz, 3rd ed., 1989.

[13] ITU-R, "Propagation data and prediction methods for the planning of indoor radiocommunication systems and radio local area networks in the frequency range 300 MHz to 100 GHz ," *Recommendation ITU-R P.1238-8*, 07-2015.

[14] www.digi.com, "Indoor path loss," application note, accessed on: 12.01.2016, Digi, 2012.